Molding Innovation

JAN. 2012

Moldex3D
Launches New Long Fiber Orientation Prediction in R11

INSIDER

GO FOR SUCCESSFUL MOLDING

Moldex3D
MOLDING INNOVATION

Moldex3D Launches New Long Fiber Orientation Prediction in R11

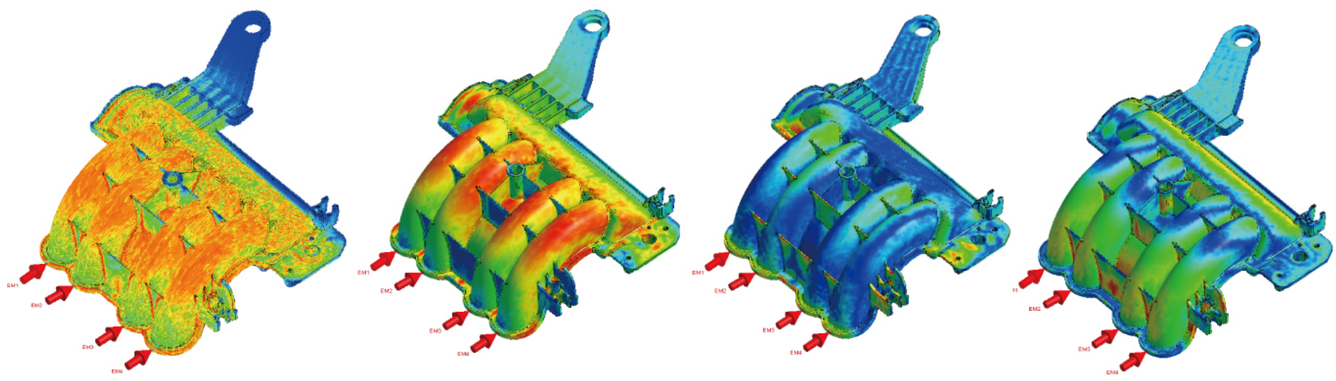

In recent years, long fibers are already widely used in automotive, consumer, and industrial applications. The practice of adding glass and carbon fibers into plastic materials reinforces the mechanical and thermal properties with little change of weight.

A qualitative relationship between the fiber length and the mechanical properties of a glass fiber reinforced plastic is shown in Figure 1. The maximum strength and the impact properties could be dramatically increased by raising the fiber length. However, these fiber-related improvements to the part's mechanical properties are heavily dependent on the fiber's orientation. For example, shear flow introduces anisotropic properties to the injection-molded parts due to the preferential orientation of fibers induced by the flow during this processing. This is ideal for a part requiring larger strength and stiffness properties in the direction along the fibers than crossing the fiber.

However, there are some cases in which random fiber distribution is desired to prevent non-uniform part warpage or shrinkage. In order to determine the performances of injection-molded parts and aid the design of the mold, part, and the processing conditions, the fiber orientation must be accurately predicted. You can find out more detailed short fiber orientation simulation validation in one of our technical papers presented in the Conference Paper section of this issue.

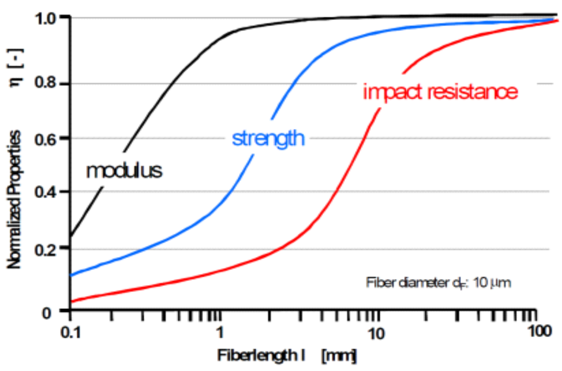

Figure1. Composite property improvement with increasing fiber length

Source : Plasticomp

Moldex3D's new long fiber orientation prediction package featured in Moldex3D R11 offers a new solution in determining the orientation of short and long fiber-reinforced thermoplastic composites. Traditional fiber orientation models using the anisotropic rotary diffusion (ARD) technique based on Folgar-Tucker model could accurately perdict the fiber orientation. However the ARD technique requires 5 parameters and an inefficient computation method. Moldex3D R11 takes a major leap forward by developing the Improved Anisotropic Rotary Diffusion (iARD) technique (US patent pending). Combined with the Retarding Principal Rate (RPR) model, the iARD model provides accurate fiber orientation prediction and fast computation times. Features include:

- Fewer parameters, users easily input only 3 iARD-RPR model parameters.
- Accelerated computations, with speeds up to 50% faster for fourth-order orientation tensor.
- Does not require experimental inlet-condition, only isotropic distribution can obtain good predictions.
- Significant characteristics of long fiber orientations considering matrix structure, fiber flexibility, and flow field.
- More accurate fiber orientation distribution and elastic modulus distribution through the part thickness.

Moldex3D's accuracy is exemplified in Figure 2, using a center-gated disk model. The A11 orientation tensors of both observed and predicted data shows a preferred orientation (large A11 value) near the wall while there is random distribution (A11 near 0) in the center. The conventional model falls short in predicting this important behavior.

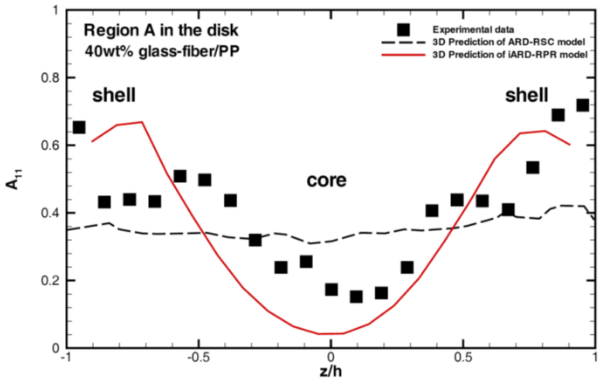

Figure 2. Moldex3D's long fiber simulation result (iARD, red line) shows an ideal agreement with observed data when compared to conventional ARD model (dotted line)

With Moldex3D's latest technology in predicting short/long fiber orientation, designers and molders can gain a better control over their product quality. For more information regarding fiber orientation demonstrations and case studies, please go to our website www.moldex3d.com to learn about our exciting new functions and applications.

INVESTIGATION OF FIBER ORIENTATION IN FILLING AND PACKING PHASES

Chih-Chung Hsu[1], *Dar-Der Hsieh*[1], *Hsian-Sen Chiu*[1], *Masashi Yamabe*[2]
1. *CoreTech System (Moldex3D) Co., Ltd., ChuPei City, Hsinchu, Taiwan*
2. *Kanazawa Institute of Technology, Ishikawa, Japan*

Abstract

Fiber-reinforced engineering materials are widely used for their superior mechanical properties in lots of plastic parts. And it is truly believed that in the injection molding process the fiber orientation and anisotropy shrinkage are very complex 3D phenomena which may influence the product properties deeply. In this research, the fiber orientation is considered both in filling and packing process numerically. The result of fiber orientation shows a good agreement with experimental data. Moreover, the investigation illustrates the strength of fiber orientation in filling and packing phases with detail.

Introduction

In recent years, the injection molding of fiber-reinforced thermoplastics has been widely used because of their superior mechanical properties in applications. The injection molding of fiber-reinforced composites is a complicated process, where the fiber-induced anisotropic mechanical properties strongly depend on the fiber orientation. The reinforced composites are stronger in the fiber orientation direction and weaker in the transverse direction; the thermal shrinkages are larger in the transverse direction and lower in the fiber orientation direction. In a result, the molded products may have high internal stress and warpage at unexpected locations. Therefore, the design of a new product must take account of processing details.

The flow-induced fiber orientation and anisotropic shrinkages in injection molding are complex 3D behaviors, which makes the properties of injected parts are difficult to be predicted. The direction of fiber orientation is full 3D components, which makes it difficult to study by the traditional 2.5D model. Thus, a true 3D injection molding simulation technique is therefore employed for obtaining the 3D distribution of fiber orientation in this study. For validation purpose, a ribbed flat plate with side gate positions is conducted by experiment to examine the effect of fibers in filling and packing process. Moreover, the anisotropic warpage behavior is also being discussed.

Governing equations

The polymer melt is assumed to behave as Generalized Newtonian Fluid (GNF). Hence the governing equations to simulate transient, non-isothermal 3D flow motion are shown as following:

$$\frac{\partial \rho}{\partial t} + \nabla \cdot \rho \mathbf{u} = 0 \quad (1)$$

$$\frac{\partial}{\partial t}(\rho \mathbf{u}) + \nabla \cdot (\rho \mathbf{u}\mathbf{u} - \boldsymbol{\sigma}) = \rho \mathbf{g} \quad (2)$$

$$\boldsymbol{\sigma} = -p\mathbf{I} + \eta\left(\nabla \mathbf{u} + \nabla \mathbf{u}^T\right) \quad (3)$$

$$\rho C_P\left(\frac{\partial T}{\partial t} + \mathbf{u} \cdot \nabla T\right) = \nabla(\mathbf{k}\nabla T) + \eta\dot{\gamma}^2 \quad (4)$$

where **u** is the velocity vector, T the temperature, t the time, p the pressure, σ the total stress tensor, ρ the density, η the viscosity, k the thermal conductivity, C_p the specific heat and $\dot{\gamma}$ the shear rate. The FVM due to its robustness and efficiency is employed in this study to solve the transient flow field in complex three-dimensional geometry.

Fiber orientation

The fiber orientation state at each point in the part is represented by a 2nd-order orientation vector A, where

$$A_{ij} = \int (p_i p_j)\varphi(p)dp \quad (5)$$

The equation of orientation change for the orientation tensor proposed by Advani and Tucker is employed for the analysis:

$$\frac{\partial A_{ij}}{\partial t} + u_k \frac{\partial A_{ij}}{\partial x_k} = A_{ik}\Omega_{kj} - \Omega_{ik}A_{kj} + \lambda\left(A_{ik}E_{kj} + E_{ik}A_{kj} - 2A_{ijkl}E_{kl}\right) + 2C_I\dot{\gamma}\left(\delta_{ij} - 3A_{ij}\right) \quad (6)$$

Where C_I is the interaction coefficient with the value ranged from 10^{-2} to 10^{-3}. In this study, we take C_I as 10^{-2} for default value. For the fourth-order tensor A_{ijkl}, a closure approximation is needed in order to calculate the distribution of 2nd order A on the basis of a velocity field. Here, the hybrid closure approximation will be primarily adopted.

Implementation details

The fiber-reinforced plastic material adopted in this study is DURANEX®3300(Grade name, written as PBT-GF in the following description). The molding condition is tabulated in Table 1. The geometry model is a ribbed flat plate with side gate positions, which is shown as Fig.1. The geometry model used to conduct the experiments is the same mold with side gate respectively. The node positions for measuring warpage behavior are illustrated in Fig. 2. The measurement results of deformation on these nodes are used to compare to simulation results. Furthermore, in order to observe the fiber orientation, the mold is divided into 20 layers in the experiment in the thickness direction, while the corresponding displayed layer number by simulation is 10. The schematic diagrams of fiber orientation for each layer using in the simulation are shown as Fig. 3 and 4.

Results and Discussions

In convenience to show the comparison of fiber orientation between experiment and simulation results, the orientation of the lines indicates the most favorable orientation direction, and the displayed color represents the degree of orientation. To clarify the fiber orientation inside the cavity, position 1~3 is investigated by three cutting plane: front, middle and back, and position 4 is done by left, center and right planes. Fig. 5~8 shows the comparison of fiber orientation between experiment and simulation results. Moreover, the simulation results in filling and packing process are also illustrated.

For observed positions 1 and 2 in Fig. 5 and 6, the evolution of fiber orientation is predicted well qualitatively as experimental result both in filling and packing process. We can see that due to the cooling effect in packing process, the polymer has solidified that there is little changes in fiber orientation. As for the front and back plane near the mold wall, the shearing flow tends to align the fibers along the flow direction. While the situation is different in the middle plane, the flow is shear free or lower and the fiber orientation no longer aligns the flow direction. Some even aligns perpendicular to the flow direction in the vicinity of the melt entrance region. However, as the melt starts developing flow pattern, the fiber continues to align to the specific directions under the effect of shear rate. This is obviously predicted as Fig. 5-(b) for distinct behavior in filling and packing process.

For observed position 3, Fig. 7 shows the fiber orientation in the end of flow line. There is some strength and direction difference in filling and packing phase. However, packing phase predicts better than filling in the phenomena that fibers tend to flip over and stand in the observed slicing plane. Observed position 4 as showing in Fig. 8 is taken to investigate the fiber orientation in the thickness direction. A simple sketch map of fiber orientation can be formed as Fig. 9. We can divide the fiber orientation distribution into three laminates, where zone A is the outermost skin with no distinct pattern of orientation. Zone B exposed the high shear rate that the fiber oriented in direction of flow. In the inner laminate zone C, medium shear rate or low shear rate may result in little orientation and even transverse to flow direction. Fig. 9 is typical in injection-molded part and can be predicted by the present analysis.

In Fig. 10, we show the numerical and experimental warpage measurement. The figure show that the trend of deformation on the nodes is in a good agreement with both experiment and simulation. Since the displacement strongly depends on the strength of fiber, an uneven distribution of fiber orientation due to flow pattern may lead the mechanical properties to be anisotropic.

Conclusions

In this research, the numerical algorithm to simulate fiber orientation is validated with corresponding experimental measurements. A ribbed flat plate with side gate is used as test models, and the comparison of the slicing fiber orientation between simulation and experiment results is in a good agreement. It is found that due to the growing layer of solidified polymer during the packing process, the fiber orientation behaves a little differently in the strength of magnitude and still keeps generally the same distribution as filling process. With the consideration of fiber orientation in packing process, the product property during the whole injection molding process is assured more. Moreover, the predicted warpage deformation values are being obtained with reasonable comparison with the experimental data under the considering of fiber orientation both in filling and packing process.

Reference

1. Michii Takayuki, Seto Masahiro, Yamabe Masashi, and Otsuka Hiroki, “Warpage Mechanism duo to Fiber Orientation during Injection Molding”, 467, Seikei-Kakou, Vol.**16**, No.7, (2004).
2. W.H.Yang, David C. Hsu, Venny Yang and R. Y. Chang, “Computer Simulation of 3D Short Fiber Orientation in Injection Molding”, 470, ANTEC 2003, Nashville, (2003)
3. R. Y. Chang, W. S. Yang, “Numerical Simulation of Mold Filling in Injection Molding Using a Three-Dimensional Finite Volume Approach.”, 125, Int. J. Num. Meth. Fluids, Vol. **37**, (2001).

Table 1 Molding conditions

Melt temperature (°C)	250
Mold temperature (°C)	60
Injection velocity (m/min)	1.0
Holding pressure (MPa)	68.6
Injection time + Holding time (sec)	10
Cooling time (sec)	20
Cycle time (sec)	40

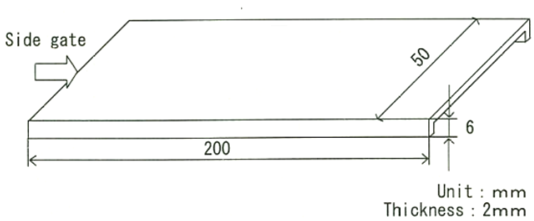

Fig.1 Geometry of mold cavity

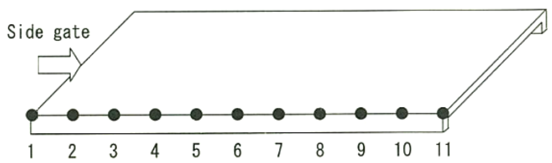

Fig.2 Measuring nodes for warpage behavior

Fig. 3 Observation Position

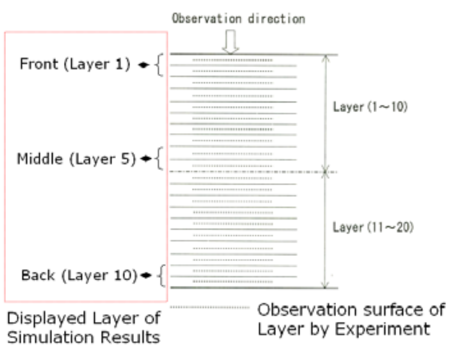

Fig. 4 Observation layers by experiment and corresponding layers by simulation.

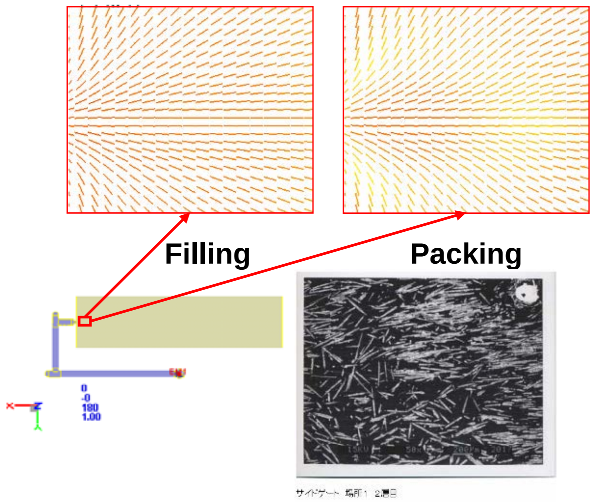

(a) Position 1: Front

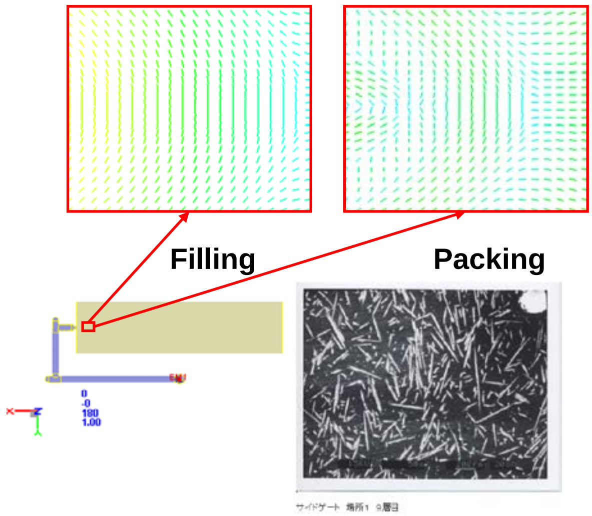

(b) Position 1: Middle

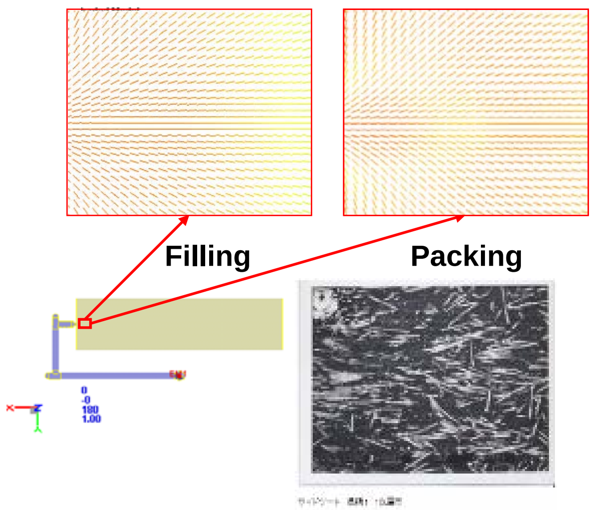

(c) Position 1: Back

Fig. 5 Fiber orientation comparison for Position 1

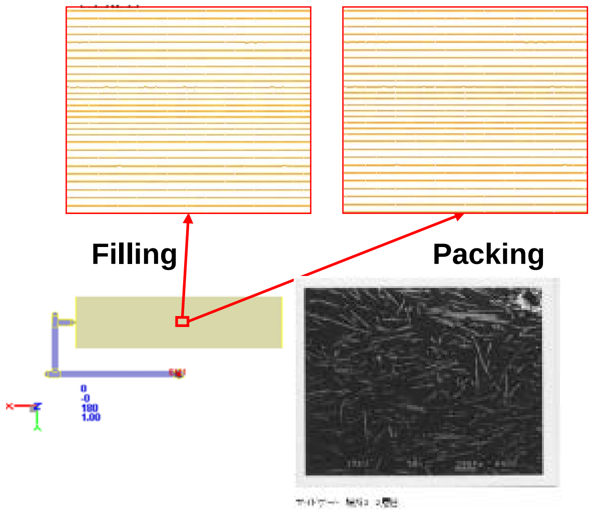

(a) Position 2: Front

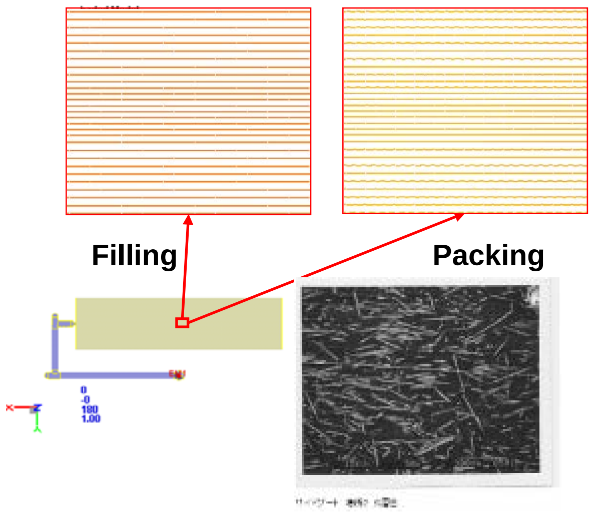

(b) Position 2: Middle

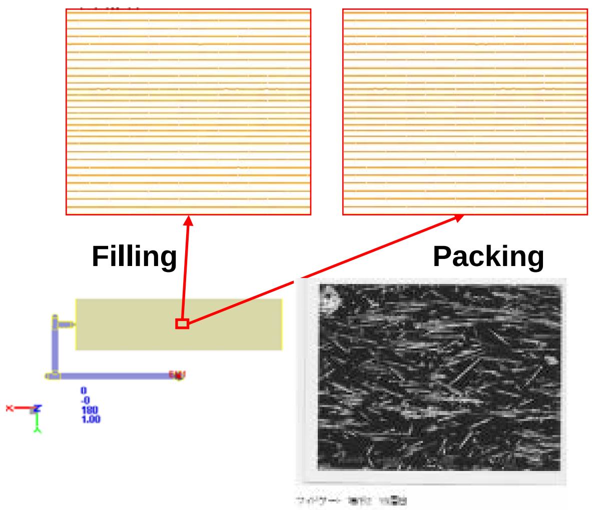

(c) Position 2: Back

Fig. 6 Fiber orientation comparison for Position 2

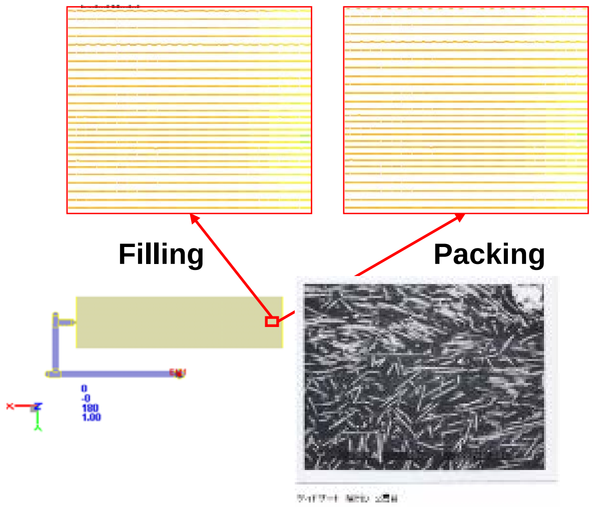

(a) Position 3: Front

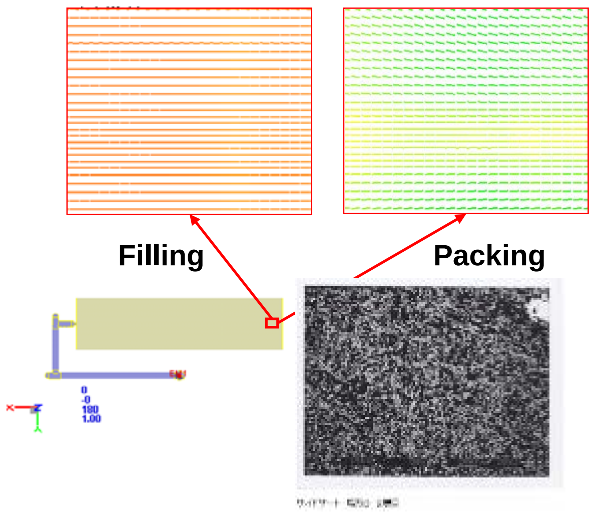

(b) Position 3: Middle

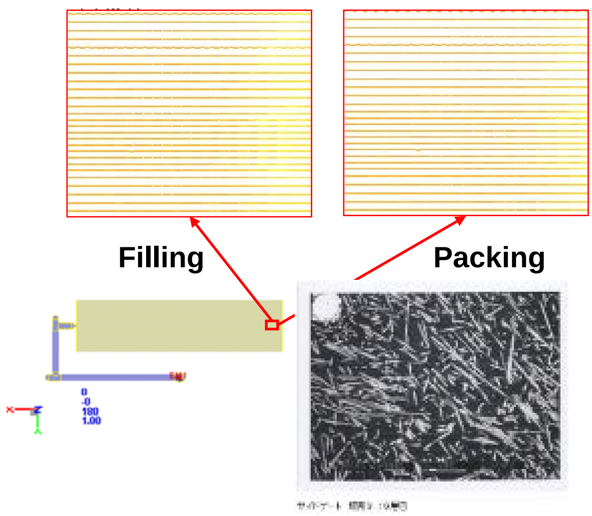

(c) Position 3: Back

Fig. 7 Fiber orientation comparison for Position 3

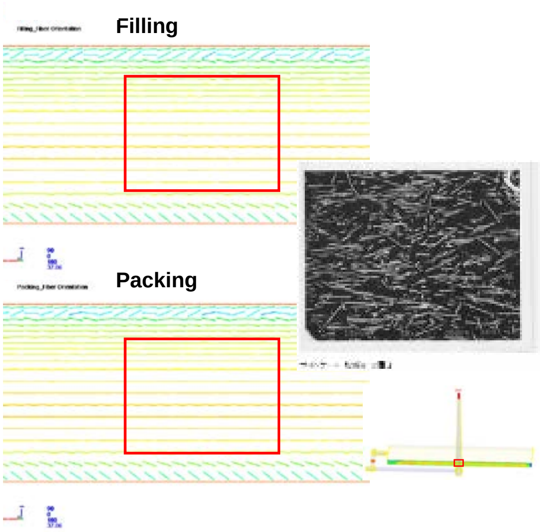

(a) Position 4: Left

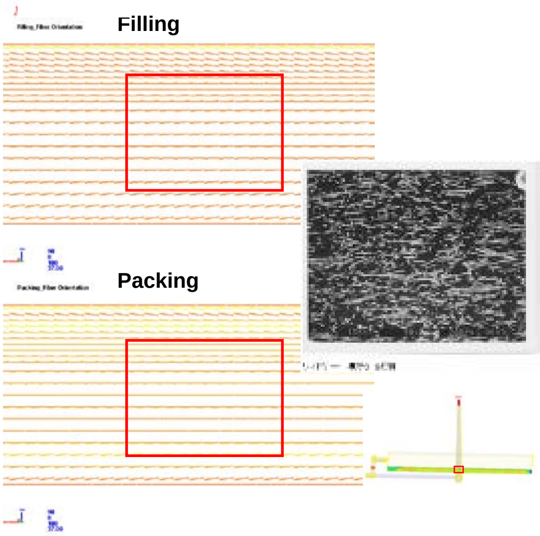

(b) Position 4: Center

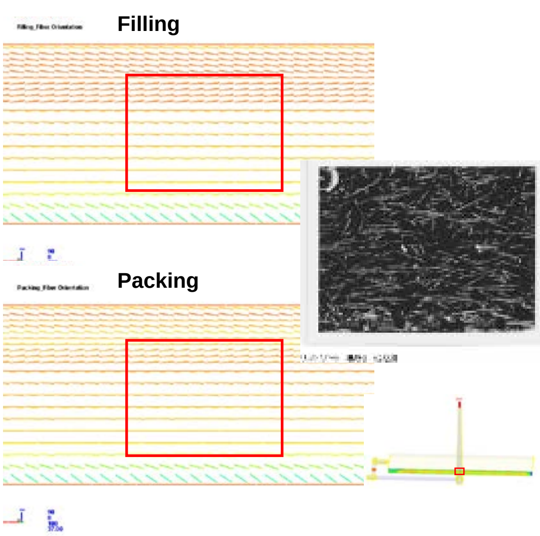

(c) Position 4: Right

Fig. 8 Fiber orientation comparison for Position 4

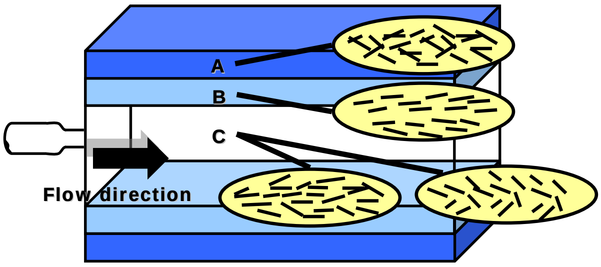

Fig. 9 Simple sketch map of fiber orientation

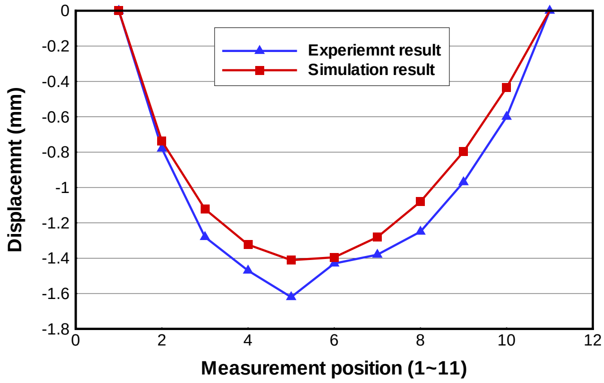

Fig. 10 The comparison of deformation between experiment and simulation results

Design Changes Made Easy With Moldex3D R11

Except for eDesignSYNC, which provides integration between eDesign and the CAD environment, eDesign itself can now perform simple geometry modifications as well. You can quickly perform design modifications without leaving the eDesign environment thanks to the new Modify Thickness function! If you are uncertain about the effect of any feature thickness change to the flow behavior, you can run multiple simulations, then select the most desirable design and lock it in. The simple procedure is as follows:

1. Import your model.

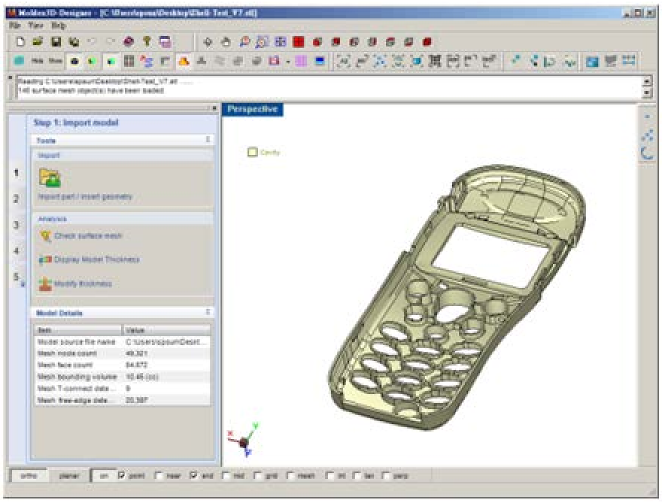

2. The new Modify thickness function is in Analysis section.

3. Once clicked, the new Modify Model Thickness menu will appear.

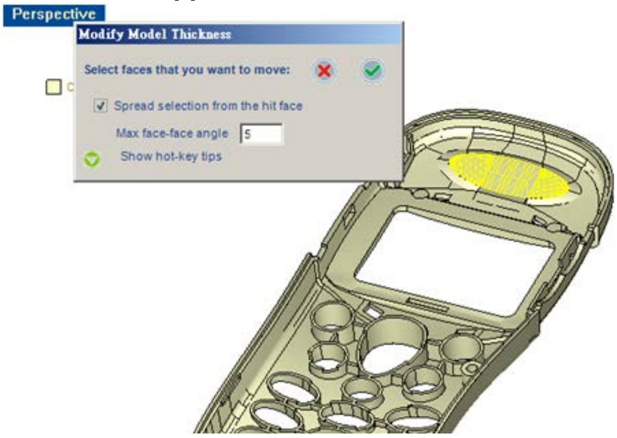

4. Choose your plane and drag it to the desired thickness, in this case 0.67 mm.

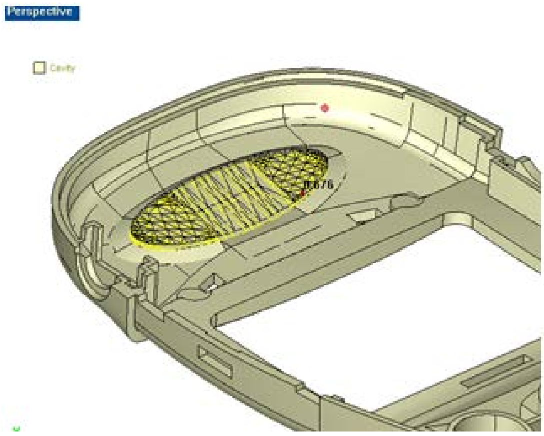

5. Voila! The thickness change in no time.

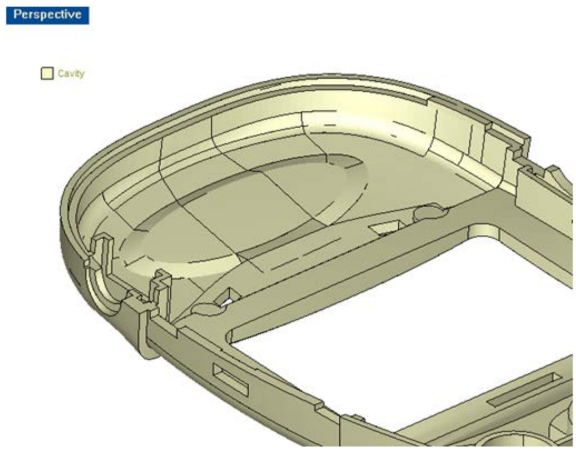

Get eDesignSYNC Instant Insight intoYour CAD

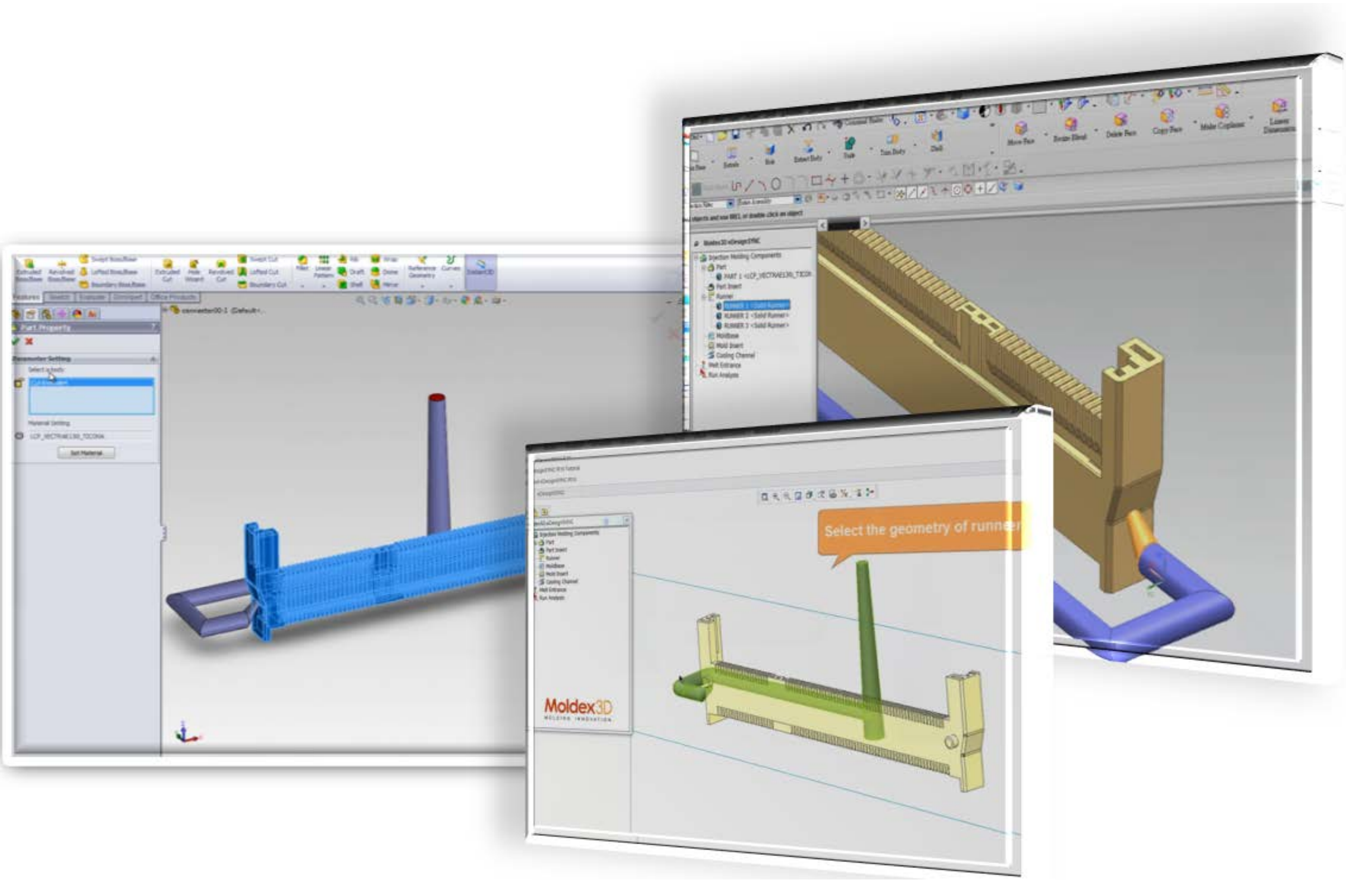

Moldex3D eDesignSYNC is seamlessly embedded within NX, Creo, and SolidWorks. With a friendly user interface and automatic 3D meshing technology, eDesignSYNC makes the simulation preprocessing easier than ever! You can finish preprocessing and setup every process parameter without leaving the CAD environment. The available analysis with eDesignSYNC includes flow, pack, cool, warp, MCM, fiber, etc. To learn more, please watch our tutorial of eDesignSYNC for NX now! The same procedures can be converted to Creo and SolidWorks.

Basic Tutorial

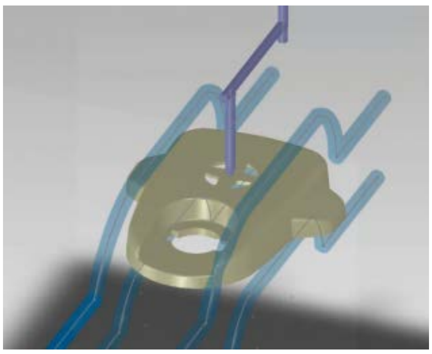

From this video, you will learn the basics of eDesignSYNC. With just a few quick steps, you can begin simulating your model.

› **Choose Your CAD to Watch:**

[NX](#) [Creo](#) [SolidWork](#)

Solid Runner & Symmetry Computation Demo

eDesignSYNC can also support the runner system created within CAD environment. With a solid runner system, you will be able to apply symmetry computation to your model. Applying symmetry computation will not only decrease the calculation time, but also raise the accuracy of the simulation.

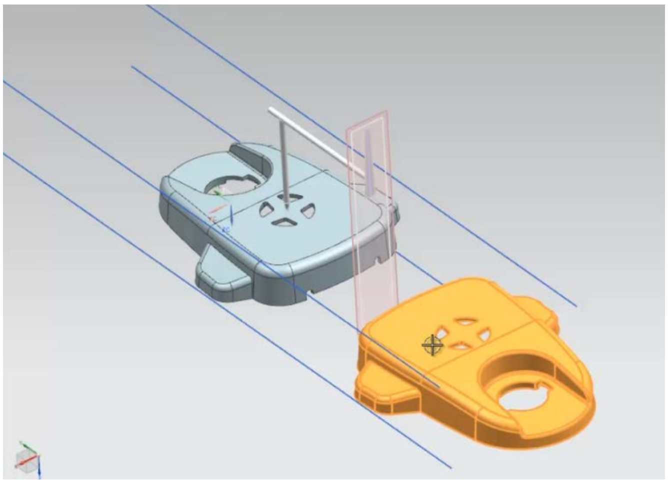

› **Choose Your CAD to Watch：**

NX Creo SolidWorks

Case Studies

Using eDesignSYNC can be cost effective to your design. Throughout these case-study demonstrations, you will learn how to discover possible manufacturing defects and then how to improve the design to avoid or eliminate the problem.

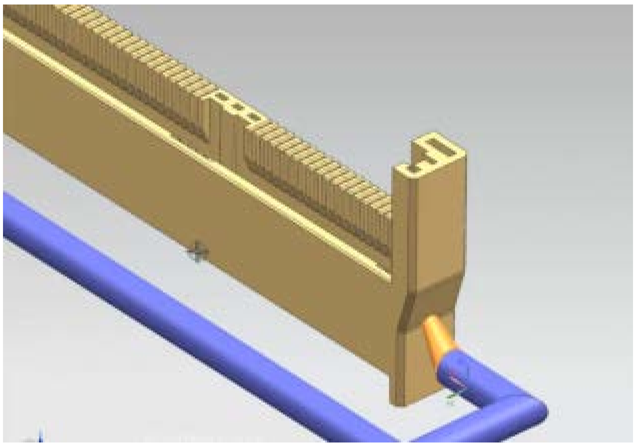

Connector

In this demonstration, a typical connector will simulated by eDesignSYNC. By examining the result of the simulation, we can easily discover that the flow pattern of the part is unbalanced. By changing the thickness of one side of the connector, the result will be improved.

› **Choose Your CAD to Watch：**

NX Creo SolidWorks

Leading Auto-parts Maker Maximized Competitiveness with Injection Molding Simulation

Founded in 1967, the Tong Yang Group is Taiwan's leading supplier of automotive components with a wide range of products. They specialize in both exterior and interior components such as: grilles, front and rear bumpers, door trims, instrument panels, center consoles, door panels and much more. By supplying both OEM corporations and aftermarket suppliers, their 2011 global revenue has grown to more than $10 billion while employing 7,200 workers worldwide.

Today, the Tong Yang Group is facing tough completion from auto part manufacturers in China and India, as well as the perpetual concern for lower costs products and services. In the past, the Tong Yang Group employed the traditional trial-and-error approach to injection molding, which was costly and time-consuming. While using the trial-and-error method, the Tong Yang Group was still expected to enhance developmental capacity to meet their customer's high standards as well as stay ahead of their completion in both cost efficiency and part quality.

The OEM Business Group collaborates with well-known automotive manufacturers to evaluate the manufacturability of their part designs. Then, based on those modeled part designs and 3D numerical analyses, the Tong Yang Group can detect potential problems and offer solutions to prevent costly setbacks.

However, in order to remain competitive in an environment that requires high versatility at low volumes, auto manufacturers are trying to differentiate themselves from the competition by enhancing their vehicle's appearance. Plastic parts such like bumpers, grilles, and aero kits are among the top priorities for appearance changes. These concerns drive the need for simulation software.

Their interior design department uses Moldex3D's simulation analysis on their plastic parts to avoid visual flaws within the part. Since the appearance of interior and exterior parts is the key focus for most consumers, aesthetic quality is paramount. Moldex3D's analysis can help predict the location of sink marks, weld lines, warpage and gaps, all of which would produce visually unacceptable, poor quality parts.

In 2000, the Tong Yang Group adopted Moldex3D's injection molding CAE software to help improve their product development. With significant part quality improvements, the company soon widened its application range. Today, the Tong Yang Group owns 13 licenses of Moldex3D's software, applying it to product designs, mold designs and outsourced vendors. Moldex3D's software offers versatile solutions to multiple departments:

- Assisting designers to understand the relationship between part design, mold design, material properties, and molding parameters.
- Lowering development costs.
- Creating product and mold design benchmarks and building learning experiences.

Optimal mold design solutions can be achieved through Moldex3D's analysis. The results can then be benchmarked and ready for cost evaluation and mold testing. Users can check whether or not the analysis results match real-world performance, and ultimately shorting mold testing time.

"CoreTech is more than an injection molding simulation software supplier. They truly understand the challenges facing the molding industry and can always provide us with real-time professional assistance," said Jeff Chien, the director of manufacturing division of Tong Yang Group.

Through continuous design process improvement, Moldex3D can help reduce cycle time by an average of 21.7 seconds for parts such as bumpers. Other products also gain great reduction in cycle time as well. "Our company's productivity has been enhanced by 21.28%, which largely increased our cost advantage. We will adopt simulation analysis among upstream design suppliers, paving the path to collaborative and optimized designs," – Mr Chien.

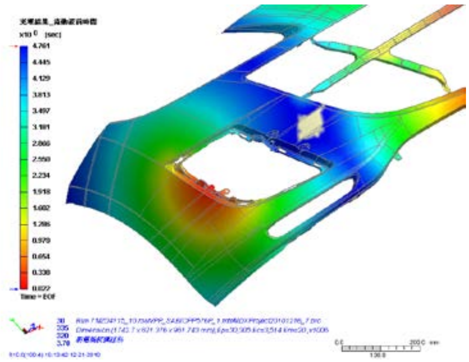

a. Prediction on air trap location opens for mold venting

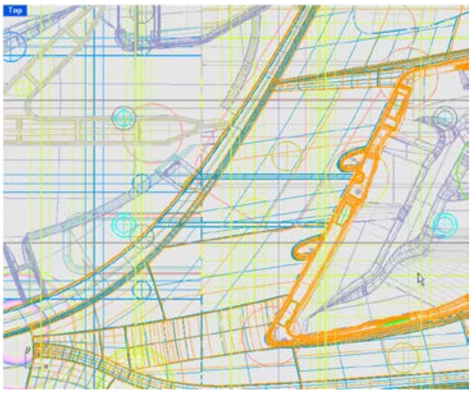

b. Place ejector pin in advance before the mold

UTAC's Report on Molded Underfill Technology Leveraged on Moldex3D and Won Best Paper of Session in IMAPS

UTAC Group is a leading independent provider of semiconductor assembly and testing services for a broad range of integrated circuits. The Group offers a full range of package and test development, engineering and manufacturing services and solutions to a worldwide customer.

The IC industry is always challenging for thinner packages with smaller footprint. Flip-chip packages have gained significant use in production over the years because of its high inputs/outputs (I/O), enhanced performance and small form factors. Though the flip-chip technology has various advantages over the other high-density electronic packaging approaches, there are rising challenges to ensure moldability and minimize defects with rapid advances in flip chip technology such as decreasing bump pitch, stand-off height, thinner package profiles and molded underfill (MUF) materials. The complexity was further exacerbated by the possible interactions between these factors and their impact on package yield, reliability andperformance. Void entrapment challenges are faced with increasingly small gap at the bumps area under the die, resulting in significant melt front imbalance and flow resistance.

UTAC has employed Moldex3D to setup a virtual molding trial laboratory since 2009. The team has applied it to numerous packaging projects successfully. "We aim to leverage Moldex3D simulation capabilities to solve key problems faced in production." said Ore Siew Hoon, the team leader. "Experiments involving a large DOE matrix are typically used to solve the molding issues, and is very time consuming and difficult because of the complex interactions between fluid flow, heat transfer and polymerization of encapsulant. Numerical simulation is an effective tool for analyzing the complicated physical phenomena", added Ore Siew Hoon. Recently, the Group's technical paper was proudly awarded the Best Paper of Session in the 44th IMAPS International Symposium on Microelectronics. The PDF file is available for reference here.

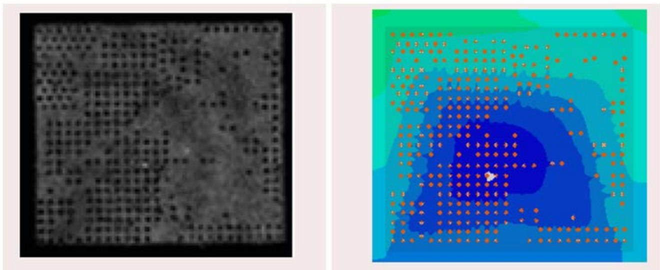

The validation shows Moldex3D accurately predicts the air entrapment in the molded underfill package.

Molding Flow Modeling and Experimental Study on Void Control for Flip Chip Package Panel Molding with Molded Underfill Technology

Jonathan Tamil[1], Siew Hoon Ore[2], Kian Yeow Gan[3], Yang Yong Bo[4], Geraldine Ng[5], Park Teck Wah[6], Dr Nathapong Suthiwongsunthorn[7], Dr Surasit Chungpaiboonpatana[8]
United Test and Assembly Center[1,2,3,4,5,6,7,8], 5 Serangoon North Ave 5 S554916,
Jonathan_Tamil@sg.utacgroup.com[1], (65) 65511386[1]

Abstract

Increasing challenges are faced to ensure moldability with rapid advances in flip chip technology such as decreasing bump pitch and stand-off height, especially when commercial Moldable Underfill (MUF) is used and in particular, during panel level molding. One key challenge faced is severe void entrapment under the die. Experiments involving a large DOE matrix, which require significant time and process resources, are typically used to solve this issue. 3D flow simulation can be used to optimize the process to reduce defects without doing actual runs. Mold flow simulation can effectively reduce the design-to-implementation cycle time, identifying key problems before actual fabrication. In this paper, 3D mold flow simulation using Moldex3D™ V10 is applied to transfer molding to optimize design and process parameters.

This paper proposes and verifies a systematic method that can save computational resources by using 2 steps analysis: simplified panel simulation and single package simulation. The initial step, simplified panel level simulation, is to optimize the process parameters to obtain balanced melt front. The second step is to study on the package level the effect of various package-scale parameters. This analysis provides a prediction of the void location and an insight on the appropriate parameters to minimize void problem. The actual voids location and size from the experiment was captured by SAT machine and short shots were obtained. For final validation, a complete panel-level flow model is built, where the process and design parameters adopted in the actual molding were implemented. The mold filling simulation showed good correlation with the experimental short shots and actual void location. With optimized parameters from the simulation used as guidelines, experimental tests were conducted and the study showed that the simulation is a useful tool to optimize the molding process.

1. Introduction

Flip-chip packages have gained significant use in production over the years because of its high inputs/outputs (I/O), enhanced performance and small form factors[1]. Though the flip-chip technology has various advantages over the other high-density electronic packaging approaches, there are rising challenges to ensure moldability and mimimize defects with rapid advances in flip chip technology such as decreasing bump pitch, stand-off height, thinner package profiles and moldable underfill (MUF) materials. The complexity was further exacerbated by the possible interactions between these factors and their impact on package yield, reliability and performance.

Transfer molding process using MUF for flip-chip devices was developed due to reduction of process steps, cycle time and cost compared with the conventional capillary underfill process. But void entrapment[2] challenges are faced with increasingly small gap at the bumps area under the die, resulting in significant melt front imbalance and flow resistance. Experiments involving a large DOE matrix are typically used to solve this issue. However, applying the conventional trial-and-error method to optimize this process is time consuming and difficult because of the complex interactions between fluid flow, heat transfer and polymerization of MUF. Hence computer-aided-engineering (CAE) is an effective tool for analyzing the complicated physical phenomena inherent in the process of encapsulation of flip chip packages. Simulation can be used to provide further insights of the underlying physics to help address the defect concerns.

In this paper, 3D mold flow modeling of the transfer molding process with MUF using Moldex3D V10 is applied to optimize design and process parameters that can reduce device defects and enhance yield. The Cross Castro-Macosko model is used to define the MUF epoxy viscosity behaviors, where its rheological parameters were acquired using parallel plate rheometer and DSC(Differential Scanning Caloriemeter). The test vehicle selected is a flip chip package with bump height of 100um.

A systematic approach is developed to address the complex flow issues. As the full panel bumped array of flip chip devices would require high computational resources and time, an initial simplified chip level simulation is used to study the effect of various parameters. This analysis provides a prediction of the void location and an insight on the appropriate parameters to minimize void problem. With the insights provided by the preliminary study, the full panel level study is conducted next to evaluate the impact of process and design parameters with the aim of obtaining a balanced melt front and minimize voids.

The actual voids location and size from the experiment was captured by SAT machine and short shots were obtained. The mold filling simulation showed good correlation of the mold fronts obtained by process short shots and actual void locations. With the successful validation of the simulation, the simulation matrix as shown in Fig.1 was designed for a comprehensive assessment of the process, design and material impact on the molding performance.

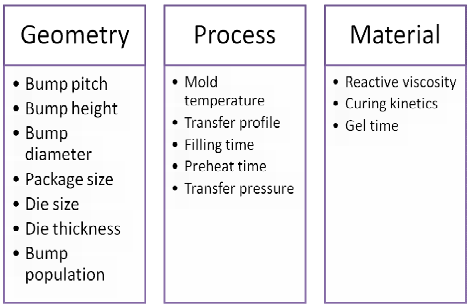

Fig.1: Rheokinetic Flow Modeling Matrix

From the rheokinetic flow modeling of MUF process, we identified the key factors and minor factors on void trapping simulation results from the extensive list of process, design and material parameters. This paper presents the valuable insights of various factors on flip chip device moldability based on process and materials used for the device. The insights can be used as upfront guidelines to predict and reduce potential product defects and failures.

With consideration of process, materials and design, this study has demonstrated that mold flow simulation is an effective tool to reduce the design-to-implementation cycle time with identification of potential void and melt front imbalance issues before actual fabrication. The simulation tool is used actively to-fro in conjunction with materials, process and design inputs and considerations, to predict the trend of various factors on moldability upfront to reduce the yield, cost and cycle time as shown in Fig.2. With our increasing range of flip chip products provided, we provide a comprehensive closed-loop solution including moldflow, thermal, mechanical and electrical studies[3] to the rising challenges faced with greater consumer demands for smaller and thinner flip-chip packages with better performance and greater functionalities.

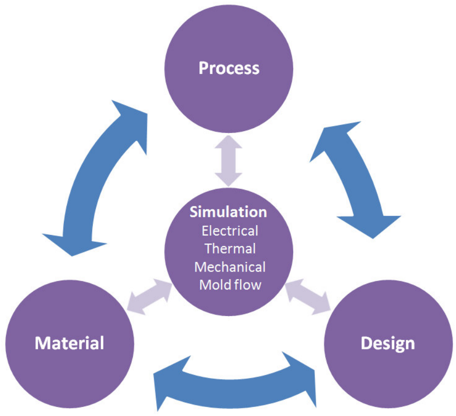

Fig.2: Closed-Loop Material, Process, Design and Simulation to Enhance Flip Chip Product Yield and Reduce Cycle Time

2. Rheokinetic Characterization of Moldable Underfill

In the transfer molding process, flow and heat transfer is dynamically coupled with the curing reaction[4]. The kinetics of the curing reaction not only affects the degree of conversion of the molding compound but also has strong effort on the mold flow with increase in viscosity due to curing reaction. Viscosity is influenced also primarily by temperature and shear rate. Therefore the rheological behavior of molding compounds is of fundamental importance for modeling of the molding process.

The MUF rheokinetic behaviors and other material properties were characterized for the flow modeling, including viscosity with varying shear rates and temperatures, curing kinetics, thermal conductivity, heat capacity and mechanical properties etc. The curing kinetics were measured using DSC with at different temperature ramp-up rates (5, 10, 20, 40°C/min). The experimental data of cure conversions were fitted by numerical parameters using the Kamal's relation [5][6] and the fitting parameters are summarized in Table I for MUF sample A. The experimental data and the numerical fitting line show good agreement, as shown in Figure 3.

$$\frac{d\alpha}{dt} = \left(k_1 + k_2\alpha^m\right)\left(1-\alpha\right)^n$$

$$k_1 = A_1 \exp\left(-\frac{E_1}{RT}\right)$$

$$k_2 = A_2 \exp\left(-\frac{E_2}{RT}\right)$$

Parameter of Kinetics	Unit	Value
M	**N/A**	**5.0467 e-1**
N	**N/A**	**1.0207**
A	**1/sec**	**1.7751 e+3**
B	**1/sec**	**1.7746 e+5**
T_a	**K**	**7.0369 e+3**
T_b	**K**	**7.0372 e+3**

Table 1. Numerical parameters using the Kamal's relation and the fitting parameters for MUF sample A

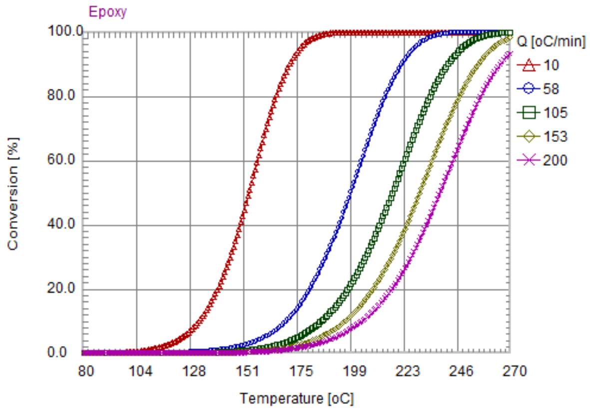

Fig 3. Curing Kinetics Curves: Conversion (%) vs Temperature

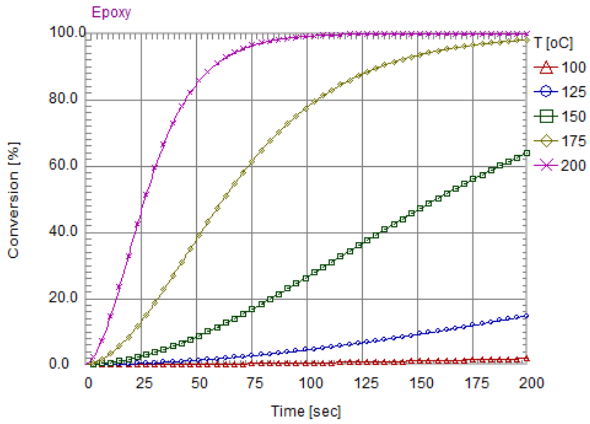

Fig 4. Curing Kinetics Curves: Conversion (%) vs Time

The viscosity is measured by the parallel plates rheometer at different temperatures ramping rates (10, 20, 40, 60 °C/min) and different shear rates (1, 2.5, 5, 10 1/s), where the viscosity changes with time. The measured viscosity is fitted by the following Cross Castro Macosko's model [7]. The experimental data set and numerical fitting results with good agreement is shown in Fig 4 and 5.

$$\eta = \frac{\eta_0}{1+\left(\frac{\eta_0 \gamma}{\tau^*}\right)^{1-n}} \left(\frac{\alpha_g}{\alpha_g - \alpha}\right)^{c_1 + c_2 \alpha}$$

$$\eta_0 = B e^{\frac{T_b}{T}}$$

	Unit	Value
n		9.683 e-2
Tau*	Dyne/cm^2	2.000 e+3
B	g/cm.sec	6.263 e-43
T_b	K	4.937 e+4
C_1		1.818
C_2		-5.521
α_g		0.25

Table 2. Numerical parameters for Cross Castro Macosko model

Where γ is shear rate, α is conversion, n is the power law index, η_0 the zero shear viscosity, τ^* is the parameter that describes the transition region between zero shear rate and the power law region of the viscosity curve.

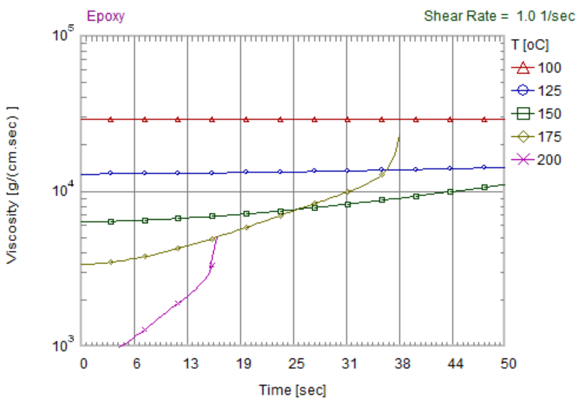

Fig 5. Viscosity Curves: Viscosity vs Time

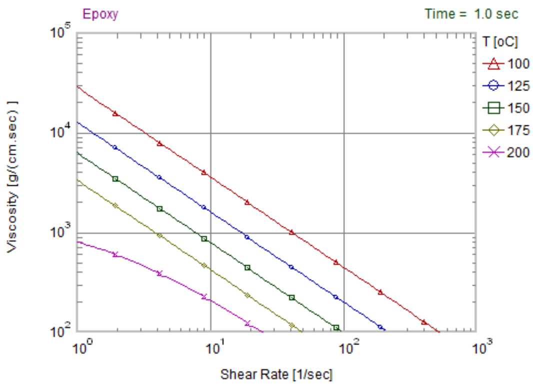

Fig 5. Viscosity Curves:
Viscosity vs shear rate

3. MUF Flow Modeling and Experimental Benchmarking

Results for Flip-chip Test Vehicle

An illustration of the transfer molding of the selected flip chip device for our current study is shown in Fig.6. The die thickness (Dt) is 0.15mm, underfill gap between substrate and die (Bh) is only 0.1mm and total mold height (Mt) is 0.53mm. There are minimum 3 mesh elements between the smallest gaps in the model. The transfer time with optimum ram speed profile control was obtained from the mold process DOE. The transfer molding process simulation is conducted using Moldex3D module for IC molding process. Actual experimental data are used in order to benchmark with our MUF flip chip transfer molding modeling.

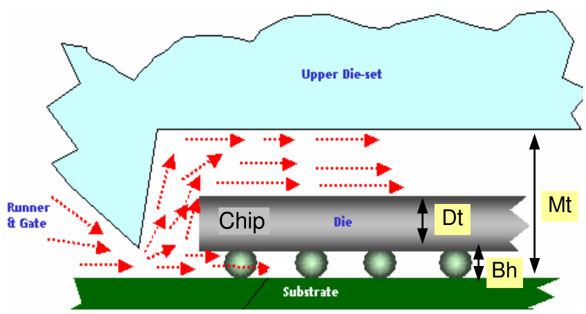

Fig. 6 Transfer molding of the selected flip chip device

The experimental short shots and simulation results are compared to assess the melt front predictions. Table 2 shows the short shots of the mold process results captured during the mold process. The comparison showed good correlation of the melt fronts obtained by process short shots with the mold filling simulation, where the melt front advancement patterns are similar to the simulated melt front contours. The melt front as observed from both short shots and simulations is generally balanced, except for slight flow retardation observed on the die areas due to flow resistance from the narrow flow channels created by the narrow gaps in these areas above the under the dies.

Short Shot Pictures	Moldflow Simulation
Transfer Time: T1	
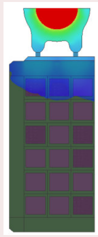	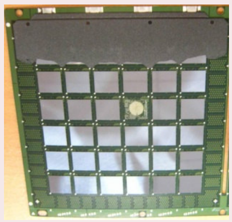
T2	
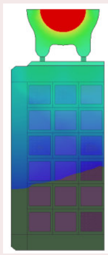	
T3	
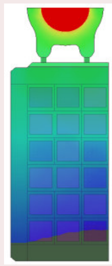	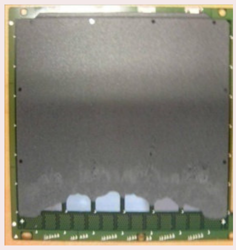

Table 2: Short Shots and
Melt Front Simulations Correlation

The actual voids location and size from the experiment was captured by scanning acoustic microscope (SAT) imaging machine. We can observe the entrapped voids in the underfill areas in selected packages on the different rows in the panel as shown in Table 3. The locations of the simulated and experimental void entraps are nearly identical. Thus the simulation showed good correlation of the actual void locations.

Voids by SAT	Moldflow Simulation
Row 1	
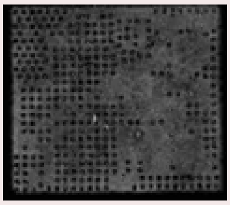	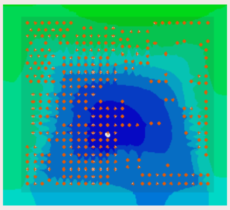
Row 2	
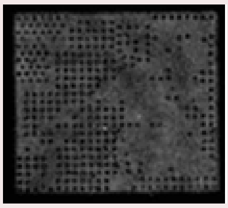	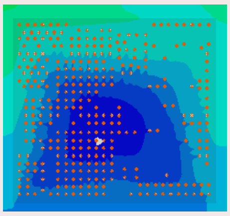
Row 3	
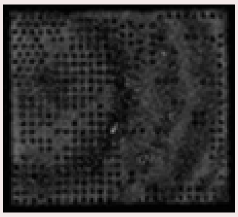	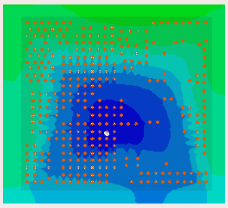
Row 4	
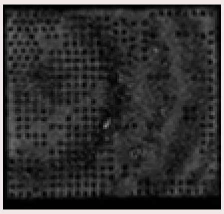	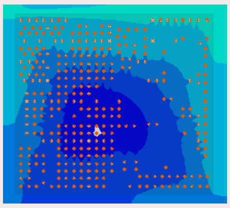

Table 2: Short Shots and
Melt Front Simulations Correlation

Fig.7 shows the simulated melt front advancement contour results for both above and under the die with the flip chip bumps. Initially, the melt front of the mold top side and bottom side are similar, but due to the presence of bumps, the melt fronts above and underneath the die are separated. The melt front near the top side of mold cavity is much faster than that of the bump area of near the substrate side where the 100μm gap is much narrower than the 280μm For this test vehicle, it is observed that the void trapping phenomena is more severe under the more densely bumped area which are next to the much less densely bumped area. The flow imbalances due to the above factors are observed to be key factors of void trapping where the two separated melt fronts are merged again.

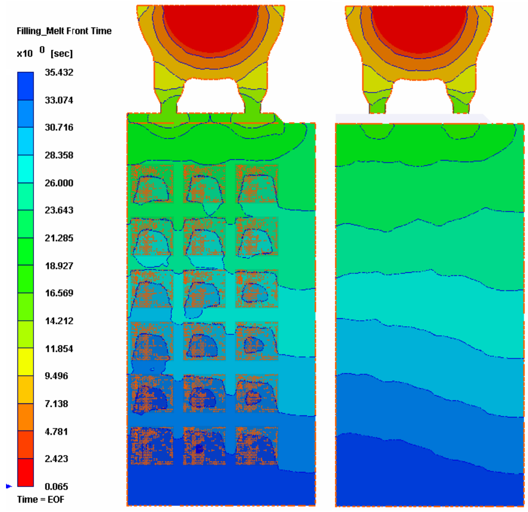

Fig. 7 Panel Level Melt Front Advancement Contours
(a) Below Die (b) Above Die

With the successful validation of the simulation, the simulation matrix as shown in Fig.1 was then studied for a comprehensive assessment of the process, design and material to enhance molding performance.

3. Systematic Evaluation of the Impact of Process and Design Parameters on Molding for a More Balanced Melt Front and Minimizing Void Issues

We have developed a systematic approach to address the complex flow issues. As the full panel bumped array of flip chip devices would require high computational resources (~7million meshes) compared to chip level study (~500,000 meshes), an initial simplified chip level simulation is used to study the effect of various package-scale parameters. This analysis provides a prediction of the void location and an insight on the key parameters to minimize the voiding problems, and overall minimize the cycle time required to obtain the results.

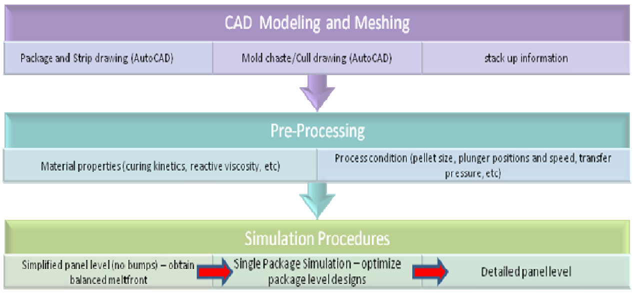

Fig. 8 Flow Chart Illustrating the Systematic Evaluation of the Impact of Process and Design Parameters on Moldability using Molding Simulation Tool Moldex3D

A. Chip Level Simulation

A simplified package 3D model with bumps is first created for an initial analysis as shown in Fig.9, with the mold filling direction as indicated by the red arrow.

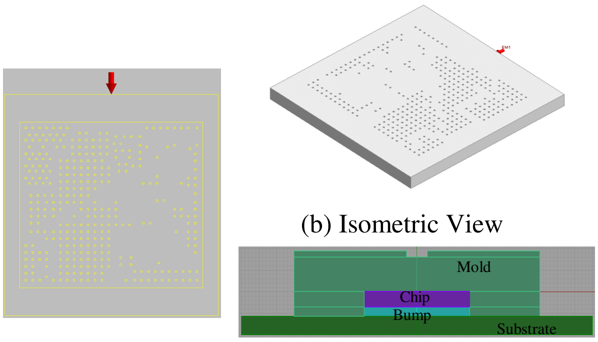

(b) Isometric View

(a) Top WireframeView (c) Side View

Fig. 9 Chip Level Simulation Model

The process parameters such as filling time and mold cavity temperature are first varied to analyze the impact of process parameter change on the molding performance using the molding simulation tool. The filling time was varied in the following two key ranges; 0.5s, 1s, 2s (much below gel time) and 10s, 20s, 30s (near gel time). The results as shown in Fig. 10 show that when the filling time is varied in the range much lower than the MUF gel time, the change from 0.5-2s results in minor impact on the void location. This may be due to the minor change in viscosity during this time range (Fig.5) and hence the minor impact on void locations. When the filling time is varied in the range near the MUF gel time, the voiding location varies, for this case shifting closer to the gate side. This could be due to the sharp change in viscosity near the gel time (Fig.5) and with the rapid change in viscosity, a more significant impact on void locations is observed. The results will vary based on the molding material used.

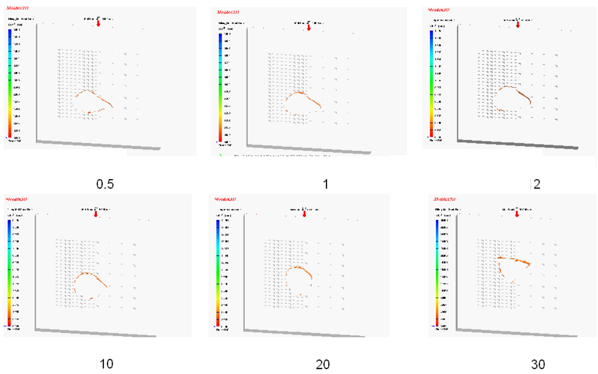

Fig. 10 Impact of Filling Time (s) on Void Location

The mold temperature was varied in the following range: 130°C, 150°C, 170°C, 190°C, 210°C. For this analysis, the filling time is 2s. The results as shown in Fig. 11 show that when filling time is in the range much lower than the MUF gel time, the change from 130°C - 210°C results in minor impact on the void location. This may be due to the minor change in viscosity during this time range, even as the temperature changes from 130°C - 210°C. The results may vary with different material and filling time used.

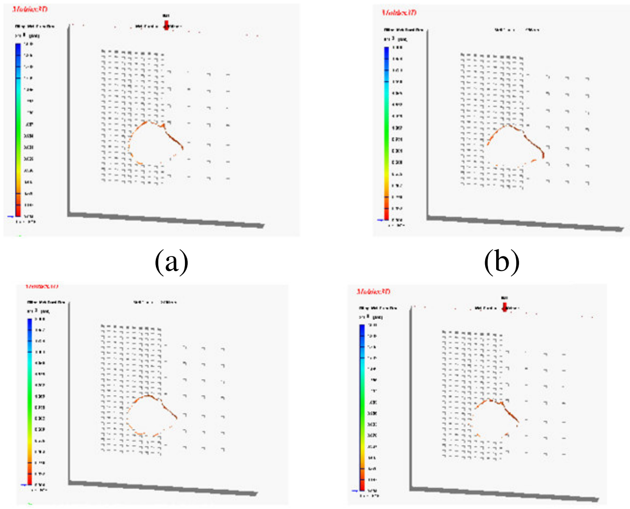

(a) (b)

(c) (d)

Fig. 11 Impact of Mold Temperature on Void Location, a) 130^{o}C, b) 150^{o}C, c)170^{o}C, and d)190^{o}C

Next, the impact of different die thickness keeping the bumps and total package height constant to conducted to study the impact of different gap sizes above and under the die on melt front. As shown earlier in Fig.7, initially, the melt front of the mold top side and bottom side are similar, but due to the presence of bumps, the layout and different in gap sizes between the die top to the mold cavity and bump height, the melt fronts above and underneath the die are separated. The melt front near the top side of mold cavity is much faster than that of the bump area of near the substrate side. The preliminary results indicate that the flow imbalances are potential key factors of void trapping where the two separated melt fronts are merged again. Due to the clearance difference above and under the die, larger flow lag is observed under the die, and we will like to investigate if voids issues reduced by creating better flow balance. Hence, two different die thicknesses as shown in Fig. 12 and Fig. 13 are studies to analyze the impact of similar gap sizes above and under the die on melt front.

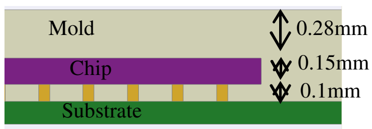

Fig 12: Chip Thickness of 0.15mm

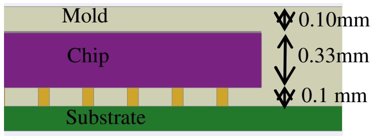

Fig 13: Chip Thickness of 0.33mm

The cross section planar cut is shown in Fig. 14 and the results of the cross sectional melt front advancements for both the thin and thick dies are shown in Fig 15 and Fig 16. The results show that the balancing the flow resistance by decreasing the gap from die top to mold cavity resulted in a more balanced melt front above and underneath the dies, reducing the voiding issues caused where the two separated melt fronts are merged again.

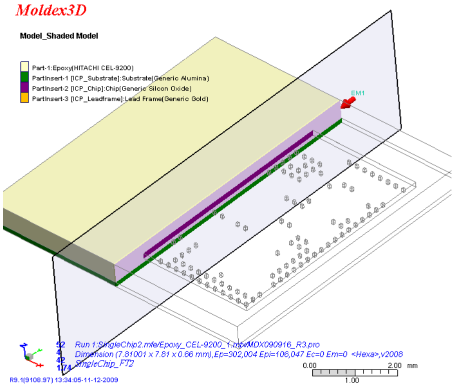

Fig 14: Cross Sectional Planar Cut for Analysis

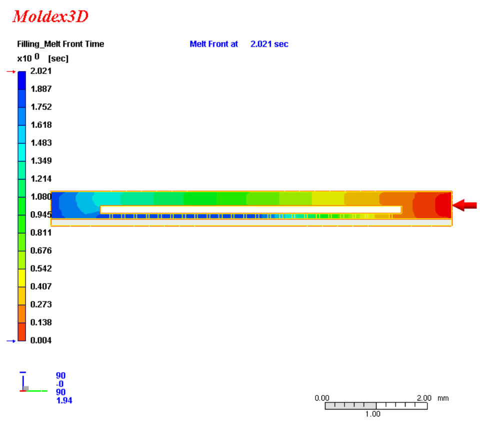

Fig 15: Melt Front Profile for Chip Thickness of 0.15mm

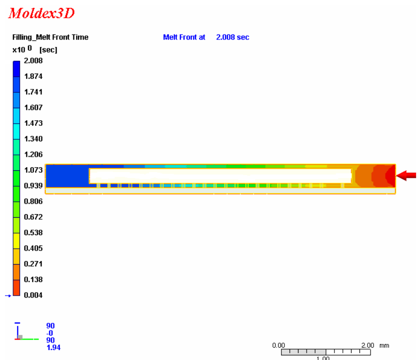

Fig 16: Melt Front Profile for Chip Thickness of 0.33mm

We also varied the bump layout to analyze the impact of different bump pitch and layout on the void locations, keeping the die thickness, bump height and total package height constant. In Fig 17, Pitch Array A has the denser bump area with pitch of approximately 0.1mm and the less dense bump area with pitch of approximately 0.6m. The results as shown in Fig 18 indicate that the different bump layout influences the location of the voids trapping. With the denser bumps area located next to the less dense bumps areas, the flow resistance caused by the denser bumps resulted in the shifting of void locations to the area with the denser bump layout. In comparison, when the bumps are evenly distributed, the void location is more centralized, though neared to the vent side with higher viscosity towards the end of filling affecting the void process.

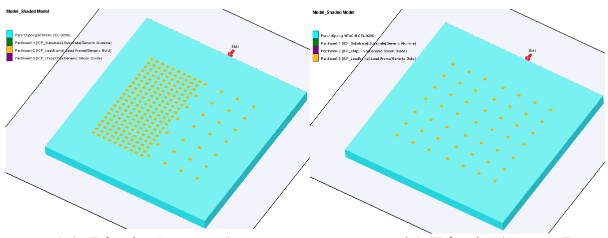

(a) Pitch Array A (b) Pitch Array B

Fig 17: Different Bump Layout Simulation Models

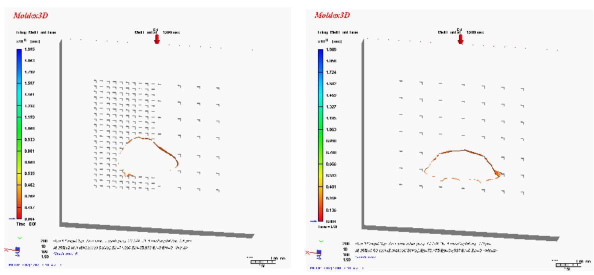

(a) Pitch Array A (b) Pitch Array B

Fig 18: Void Locations for Different Pitch Arrays

The bump height is also varied to analyze the impact of different bump height on the void locations, keeping the die and mold thickness constant. As shown in Fig 19, two different bump heights were evaluated; 0.1mm and 0.06mm, shown in Fig 19(a) and Fig 19(b) respectively. The bump layout used is Pitch Array A as shown in Fig 17(a). The results as shown in Fig 20 and Fig 21 indicate that the bump height has an impact on the location of the voids trapping. With the smaller bump height of 60µm while keeping the other factors constant, the flow resistance of the bump area near the substrate side is increased compared to the larger smaller bump height of 100µm. Hence the melt front separation for the device with smaller bump height of 60µm above and underneath the die is more pronounced. The melt front near the top side of mold cavity is much faster than that of the bump area of near the substrate side when bump height is smaller, resulting in voids trapped nearer to the gate side where the two separated melt fronts are merged again.

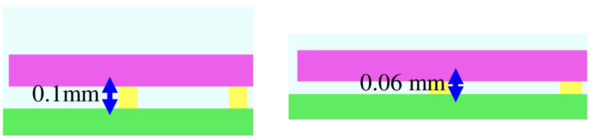

(a) Bump Height 1 (b) Bump Height 2

Fig 19: Void Locations for Different Bump Height

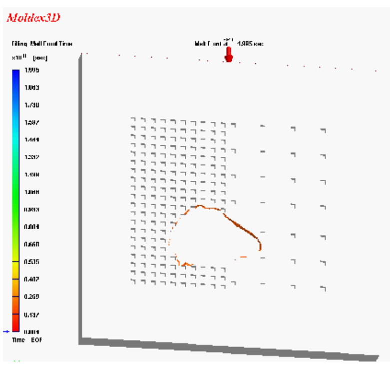

Fig 20: Void Locations for Bump Height 1 (0.1mm)

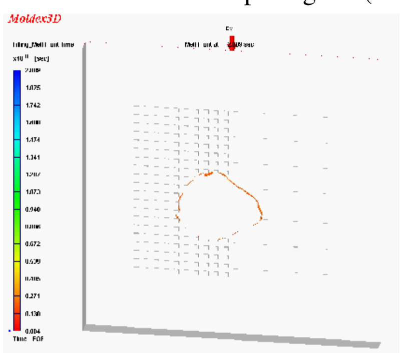

Fig 21: Void Locations for Bump Height (0.06 mm)

With the insights provided by the preliminary study, the full panel level study is conducted next with the aim of obtaining a balanced melt front and minimizes voids in the most efficient way.

B. Panel Level Simulation

The panel level simulation model is shown in Fig. 23. The total number of finite element meshes used for full panel 3D model for the current study is about 7 million, compared to 500,000 meshes for the chip level study. Analysis was also conducted to ensure that the trends for the single chip are representative of panel level studies for this selected test vehicle and conditions. From our findings, the identified trends of the single chip analysis are representative and insights useful for the subsequent full panel analysis for this test vehicle under the investigated conditions.

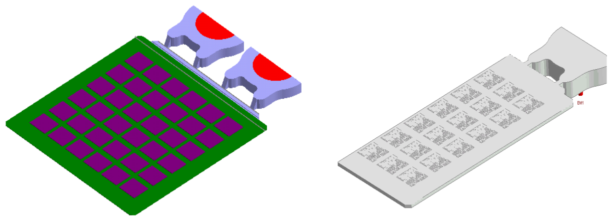

(a) Panel Solid Model (b) Panel Wire Frame Model

Fig. 22 Panel Level Simulation Model Isometric View

For the panel level analysis, we varied the chip orientation and study its impact on the void location for this test vehicle. Two different chip orientations were analyzed as shown in Fig. 24 (a) and (b).

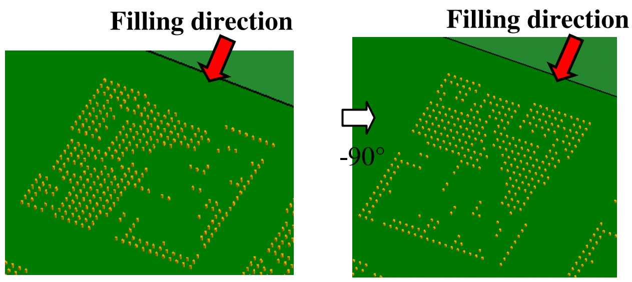

(a) Chip Orientation A (b) Chip Orientation B

Fig. 23: Panel Level Simulation Model for Different Chip Orientation

The results of the two different chip orientations on the melt front advancements and potential void locations are shown below in Fig 23, Fig 24 and Fig 25. From the results, we observed that different chip orientation resulted in different mold filling trends. For chip orientation A, the denser bump area on the right resulted higher flow resistance, where the melt fronts merged at the area of the denser bumps area, and the potential voids location shifting towards the denser bump area. For chip orientation B, the denser bump area on top towards the gate side resulted in flow retardation at that area and melt fronts merging nearer to the center of the chip compared to the chip orientation A where the voids are located nearer to the vent side. The results are also shown both for the panel view for both chip orientations as shown in Fig 24 and Fig 25.

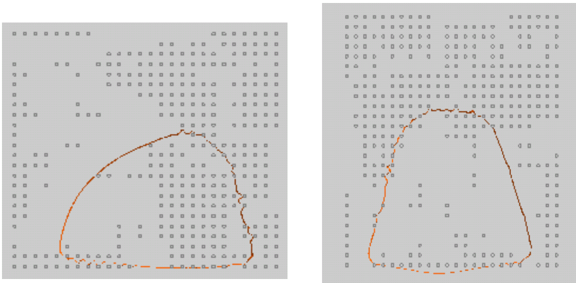

(a) Chip Orientation A (b) Chip Orientation B

Fig. 23: Melt Front on a Package on the Panel for Different Chip Orientation

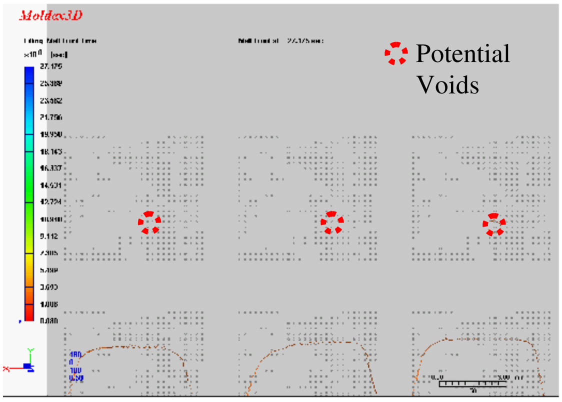

Fig. 24: Melt Front on First Two Rows on the Panel for Chip Orientation A

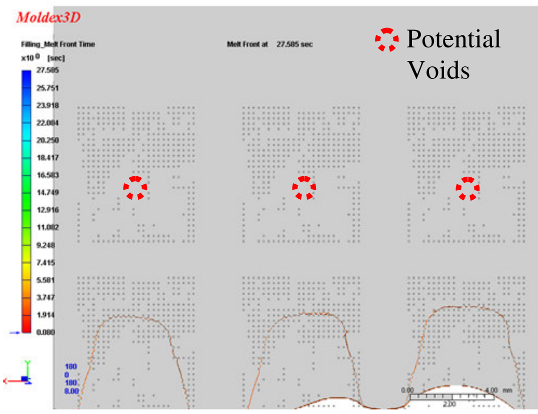

Fig. 25: Melt Front on First Two Rows on the Panel for Chip Orientation B

4. Conclusions

This paper has demonstrated our 3D mold flow modeling capability of the transfer molding process for flip chip devices with MUF using Moldex3D V10. The full MUF rheokinetic behaviors and other material properties were characterized for the flow modeling. The full panel molding simulation was conducted and compared with actual voids locations captured by SAT machine and short shots. The mold filling simulation showed good correlation of the mold fronts obtained by process short shots and actual void locations. With the successful validation of the simulation capability, the tool is then applied to optimize design and process parameters to enhance flow balance, reduce voiding problems and device defects.

To address the complex flow issues with multiple interactive factors, we designed a systematic approach to tackle the problems. An initial simplified chip level simulation is used to provide insights on the key parameters to minimize void problem. With the insights provided by the preliminary study, the full panel level study is conducted next to evaluate the impact of process and design parameters with the aim of obtaining a balanced melt front and minimize voids. Such an approach will reduce the computational resources and total cycle time required to provide mold flow solutions.

From the rheokinetic flow modeling of MUF process, we identified the key factors and minor factors on void trapping simulation results from the extensive list of process and design parameters for this study; including filling time, mold temperature, different gap sizes above and under the die, bump pitch, bump layout, bump height and chip orientation. These insights can be used as upfront guidelines to predict and reduce potential product defects and failures.

With consideration of process, materials and design, we have demonstrated that mold flow simulation is an effective tool to reduce the design-to-implementation cycle time with identification of potential void and melt front imbalance issues. With our increasing range of flip chip products provided, we provide a comprehensive closed-loop solution including moldflow, materials, process, thermal, mechanical and electrical studies [3] to address the rising challenges faced with greater consumer demands for better performance and greater functionalities.

Acknowledgments

The authors of this paper would like to acknowledge and thank the many unnamed contributors that made this capability establishment possible. These include Phaedra Fang, Goran Liu, Sam Hsieh, Ivy Hsu, Oliver Tsai, CT Huang, Dr Venny Yang and other members of the Coretech System Co., Ltd., who provided excellent moldflow tool support. I also wish to extend my appreciation to Dr Zhu WenHui and Dr Tang Gong Yue who provided support in the initial phase of this project. Lastly and most importantly, I want to express my heartfelt thanks to the UTAC management, cross functional team members and my team mates who built this capability together.

References

1. Zhuqing Zhang and C. P. Wong, "Recent Advances in Flip-Chip Underfill: Materials, Process, and Reliability" IEEE Transactions on Advanced packaging, Vol. 27, No. 3, pp 515-524, 2004.

2. Min Woo Lee, et. al. "A Study on the Rheological Characterization and Flow Modeling of Molded Underfill (MUF) for Optimized Void Elimination Design," Proceedings of the 2008 Electronic Components and Technology Conference (ECTC), Lake Buena Vista, Florida, May 27-30, pp. 382-388, 2008.

3. Siew Hoon Ore, Edith Poh S W, Dr. W.H. Zhu, Dr W.L. Yuan, Dr Nathapong Suthiwongsunthorn, "Co-Design for Thermal Performance and Mechanical Reliability of Flip Chip Devices", Proceedings of the 2010 Electronic Packaging Technology & High Density Packaging (ICEPT-HDP), Aug 16-19, pp. 81-87, 2010.

4. Nguyen, L.T, "Reactive Flow Simulation in Transfer Molding of IC Packages," Proceedings of the 1993 Electronic Components and Technology Conference (ECTC), Orlando, Florida, Jun 1-4, pp. 375-390, 1993

5. M.R. Kamal and M.R. Ryan, "Injection and Compression Molding Fundamentals," chap. 4, A.I.Isayev (Ed.), Marcel Dekker, 1987.

6. M.R. Kamal and M.R. Ryan, "Reactive Polymer Processing: Techniques and Trends,' Advances in Poymer Technology, 4, pp. 323-348, 1984.

7. J. M. Castro, and C. W. Macosko, ''Kinetics and Rheology of Typical Polyurethane Reaction Injection Molding Systems,'' SPE Technical Paper, Vol. 26, pp. 434–438, 1980.